R. A. Schneider, T. L. Naing, T. O. Rocheleau, and C. T.-C. Nguyen, "Gap reduction based frequency tuning for AlN capacitive-piezoelectric resonators," *Proceedings*, IEEE Int. Frequency Control Symp., Denver, Colorado, April 12-16, 2015, pp. 700-705, DOI: 10.1109/FCS.2015.7138938.

Gap Reduction Based Frequency Tuning for AlN Capacitive-Piezoelectric Resonators

Robert A. Schneider, Thura Lin Naing, Tristan O. Rocheleau, and Clark T.-C. Nguyen
EECS Department, University of California, Berkeley, CA/USA
Email: schneid@berkeley.edu

***Abstract*—A voltage controlled resonance frequency tuning mechanism, capable of effecting 1,500 ppm frequency shifts or more, is demonstrated for the first time on an AlN capacitive-piezoelectric resonator. The key enabler here is a compliant top electrode suspension that moves with applied voltage to effectively vary capacitance in series with the device, hence changing its series resonance frequency. Capacitive-piezoelectric AlN micromechanical resonators, i.e., those with electrodes not directly attached to the piezoelectric material, already exhibit high Q-factors compared to attached-electrode counterparts, e.g., 8,800 versus 2,100 at 300 MHz; are on/off switchable; and, as shown in this work, can exhibit electromechanical coupling C_x/C_0 of 1.0%. This new ability to tune frequency without the need for external components now invites the use of on-chip corrective schemes to improve accuracy or reduce temperature-induced frequency drift, making an even more compelling case to employ this technology for frequency control applications.**

I. Introduction

RF-MEMS resonators have seen widespread adoption in timing and wireless communications, for which the high Q's and compact form factors of such devices have enabled transformative improvements in low-power integration. Capacitive-gap resonators achieve the ultra-high Q's (exceeding 100,000) and voltage controlled tunability desired for direct RF-channelization and low phase-noise reference oscillators, yet they typically exhibit weaker electromechanical coupling than is desired at frequencies exceeding 100 MHz. Piezoelectric resonators, on the other hand, achieve the strong coupling desired for low-power oscillators and wide-bandwidth filters; however, they do so with reduced Q's of ≈2,000 and a lack of built-in tunability. An RF-MEMS resonator technology possessing integrated tuning that is capable of both very high Q and strong coupling is of great interest. In particular, commercially successful aluminum nitride (AlN) resonators would benefit from two key improvements: higher Q and integrated tuning. Voltage controlled frequency tuning of AlN micromechanical resonators allows one to compensate unwanted resonance frequency shifts due to either temperature or manufacturing variations, thus ensuring proper operation. Although numerous frequency tuning methods have been demonstrated, none simultaneously achieves integration of the tuning element and the resonator, negligible DC power consumption, and continuous (non-discrete) tuning.

Frequency tuning through microscale ovenization, even using optimized thermally isolating supports, consumes significant DC power. Such devices also require thermal codesign of a heater and resonator. The work of [1] consumes up to 2.8 mW of DC power to achieve a broad tuning range of ≈4,500 parts per million (ppm) on an AlN micromechanical resonator. Although the tuning range is sufficient, the mW-level power consumption of ovenization is undesirable for ultra-low power portable applications.

As another approach, AlN FBAR oscillators can be tuned through adding capacitance in parallel with the FBAR to reduce parallel resonance frequency, f_p. The work of [2] uses two parallel switched capacitor banks in a Pierce oscillator topology to tune f_p according to a digital control word to effect very wide frequency shifts, up to 7,250 ppm, while sustaining oscillation, attributable to an AlN FBAR's large C_x/C_0 of $\approx 5\%$. Although switched capacitor tuning in CMOS is readily suitable for tuning a large FBAR with a low capacitance tuning sensitivity, attofarad-level unit capacitance would be needed for VHF contour mode resonators given their much smaller typical sizes.

Varactor based tuning, in contrast, offers a continuous range of voltage controlled tuning capacitance, albeit with a smaller tuning ratio, C_{max}/C_{min}, than is achievable in CMOS using switched-cap tuning. The work of [3] reports varactor based frequency tuning of AlN as an improvement over ovenization citing the advantage of virtually zero power consumption. Here, an off-the-shelf varactor is connected to one or more electrodes of a 13 MHz resonator to effectively stiffen the device and increase its series resonance frequency f_s. The varactor-tuned resonators achieve ≈600 ppm of frequency tuning when one tuning electrode is used (out of four) and ≈1,500 ppm when two tuning electrodes are used. Notably, these tuned devices have rather large motional capacitances C_x's and tuning capacitances C_{min}'s of several fF and several pF, respectively, due to their operating frequency. To increase resonance frequencies towards VHF and UHF, such resonators, and hence their varactors too, would need to be scaled down in size dramatically, and would thus need very tight integration of tuning elements and resonators to mitigate parasitics, e.g., either by flip-chip bonding or co-fabrication on the same die. Since contour mode resonators are advantageous primarily due to their layout-defined resonance frequencies, one can envision a multi-frequency system utilizing corrective capacitive tuning on many such resonators, for which numerous variable capacitors, varactors or otherwise, would be needed, consuming considerable space or chip area. Indeed, it would be preferable if the variable capacitor were integrated into the resonator itself.

978-1-4799-8866-2/15/$31.00 ©2015 IEEE

II. Integrated Capacitive Frequency Tuning of Capacitive-Piezo Resonators

Capacitive-piezoelectric AlN micromechanical resonators, i.e., those with electrodes not directly attached to the piezoelectric material, offer an important value proposition: higher Q's by eliminating electrode damping [4] [5]. Such devices already exhibit high Q's compared to attached-electrode counterparts, e.g., 8,800 versus 2,100 at 300 MHz; are "on/off" switchable [6]; and (as shown in this work) can exhibit respectable electromechanical coupling C_x/C_0 of 1.0%.

Fig. 1 depicts a tunable 300 MHz radial contour mode capacitive-piezo resonator, including its mode shape and dimensions. During operation, an electric field due to an ac voltage applied across top and bottom electrodes induces strain in the piezoelectric disk, which, for an electrical signal at the resonator's natural frequency of vibration, excites the device into resonance. Interestingly, introducing top and bottom gaps g_t and g_b, and hence series capacitances C_{gt} and C_{gb}, above and below the resonator also imparts a gap dependent frequency shift to the resonator, as is discussed in Section III. This work reports the first experimental demonstration of frequency tuning via the voltage controlled reduction of either g_b or g_t. The key enabler here is a new, more compliant top electrode suspension, the design of which is discussed in Section IV, that allows for vertical actuation of the top electrode.

Fig. 2 presents the voltage-controlled top electrode pull-down phenomena used to tune series resonance frequency via the cross sections of (a) an untuned and (b) a tuned capacitive piezoelectric AlN radial contour mode disk resonator. The AlN disk, shown in dark gray, is suspended between a pair of top and bottom polysilicon electrodes, shown in light gray, by a central stem. The top electrode, which appears to be floating in the illustrations, is supported by the compliant suspension utilizing folded beams of Fig. 1. To tune the device, an applied bias voltage V_{tune} generates an attractive force between the electrodes that pulls down the top electrode, as is illustrated in Fig. 2b. The reduced gap increases series capacitance C_{gt}, thereby decreasing the series resonance frequency, f_s.

The integrated tuning method of this work eliminates the need for external tuning components and intrinsically provides the appropriate variable capacitance range necessary to properly tune a device, even as devices are scaled in size and frequency. This new ability to tune frequency without the need for external components now invites the use of on-chip corrective schemes to improve accuracy or reduce temperature-induced frequency drift, making an even more compelling case to employ this technology for frequency control applications.

III. Lumped Element Modeling

Fig. 3 presents two equivalent circuit models for a capacitive-piezo resonator. First, in Fig. 3a, sandwiched between the two gap capacitors, C_{gt} and C_{gb}, is an electromechanical representation of an AlN resonator, consisting of resonator capacitance $C_{0,ng}$ ($_{ng}$ denotes "no gaps"); an electromechanical transformer with transduction factor η; and

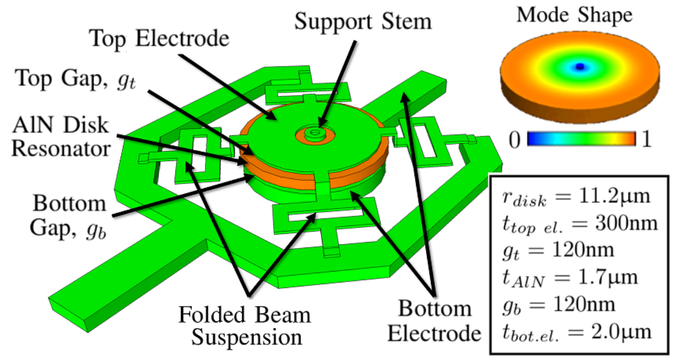

Fig. 1: Illustration, mode shape, and dimensions for a frequency tunable 300 MHz capacitive-piezo disk resonator. In this work, the resonator's top electrode suspension is made more compliant by adding folded beam supports to enable tuning.

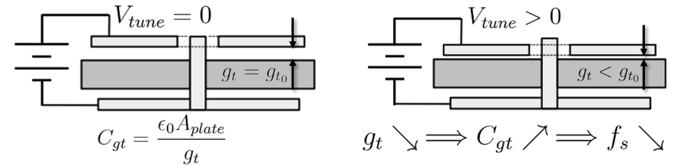

(a) An untuned capacitive piezo disk resonator for which $V_{tune} = 0$ and for which top electrode vertical displacement is zero.

(b) A tuned resonator for which $V_{tune} > 0$. Descent of the top electrode increases series capacitance, C_{gt}, and decreases series resonance frequency, f_s.

Fig. 2: Cross sections of an (a) untuned and a (b) tuned capacitive-piezoelectric AlN radial-contour-mode disk resonator. Here, the top gap g_t is reduced by V_{tune}.

mass, inverse stiffness, and damping elements l_x, c_x, and r_x, respectively. One can show that this circuit is behaviorally equivalent to the circuit of Fig. 3b having Butterworth Van Dyke (BVD) circuit component values, C_0, L_x, C_x, and R_x. To account for the changes introduced by capacitive gaps, two factors α and β are introduced to modify the component values, given by:

$$\alpha = \frac{V_{AlN}}{V_{in}} = \frac{C_g}{C_g + C_{0,ng}} = \frac{t_{AlN}}{t_{AlN} + \epsilon_{r,AlN}(g_b + g_t)} \quad (1)$$

$$\beta = \sqrt{\frac{C_g + C_{0,ng} + c_x\eta^2}{C_g + C_{0,ng}}} = \sqrt{1 + \frac{C_{x,ng}}{C_g + C_{0,ng}}} \quad (2)$$

Here, α in Eq. (1) is the factor by which input voltage in the piezoelectric is reduced by the gaps through capacitive division. In Eq. (1), C_g is the series equivalent of C_{gt} and C_{gb}. In our devices, for which g_b and g_t are 120 nm and AlN thickness, t_{AlN}, is 1.7 µm, $\alpha \approx 43\%$. β in Eq. (2) is the factor by which f_s is tuned, affecting the motional capacitor, C_x, of Fig. 3b. Here, β is slightly greater than one and depends on total gap size. Both α and β approach one as g_t and g_b drop to

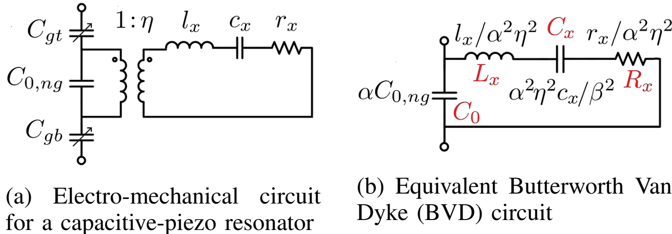

(a) Electro-mechanical circuit for a capacitive-piezo resonator

(b) Equivalent Butterworth Van Dyke (BVD) circuit

Fig. 3: Equivalent models for a capacitive-piezo resonator.

zero. Solving the BVD circuit for the frequency of minimum impedance, f_s takes the form:

$$f_s = \frac{1}{2\pi}\sqrt{\frac{1}{L_x C_x}} = f_{s,ng}\beta = f_{s,ng}\sqrt{1 + \frac{C_{x,ng}}{C_{0,ng} + C_g}} \quad (3)$$

Note that as C_g drops from infinity to zero, f_s rises between the natural eigenfrequency of the resonator $f_{s,ng}$ and the gap independent parallel resonance frequency f_p. The electromechanical coupling, $k_{eff}^2 = C_x/(C_0 + C_x) \approx C_x/C_0$ of this circuit, a performance metric gauging both maximum fractional resonator tuning range and fractional filter bandwidth, derives from the relationship between f_p and f_s as follows:

$$f_p = f_s\sqrt{1 + \frac{C_x}{C_0}} \rightarrow \frac{C_x}{C_0 + C_x} = \frac{f_p^2 - f_s^2}{f_p^2} = k_{eff}^2 \quad (4)$$

IV. Top Electrode Suspension Design

The top electrode suspension is designed to do the following: (a) have a low enough stiffness to enable reasonably low tuning voltages; (b) allow for vertical movement of the top electrode while ensuring uniform displacement over the plane of the electrode; (c) have minimal degrees of freedom to avoid unwanted rotations; (d) have a low enough electrical resistance to avoid loading Q; (e) be compact enough to allow multiple $\lambda/2$-coupled devices to exist side-by-side with each having its own suspension; and (f) have lithographically resolvable critical features. Meeting these requirements, the design of Fig. 4a was chosen and its suspension was FEM simulated to determine its displacement profile in response to a distributed force. One notes that design criterion (b) is met since the coloring of the circular plate, which indicates its vertical displacement, is quite uniform. The suspension consists of four axially-symmetric folded-beam springs and is entirely contained within the desired compact form factor. Using finite element analysis, the vertical stiffness of the device, k_z, is calculated to be 89 N/m. To predict gap tuning as a function of V_{tune}, one solves Eq. (5):

$$F_z(u_z) = \frac{1}{2}\frac{\mathrm{d}C_g}{\mathrm{d}u_z}V_{tune}^2 = k_z u_z \quad (5)$$

Through plotting gap size vs. V_{tune} as is shown in Fig. 4b, the voltage at which electrode to resonator contact occurs is predicted to be 24V. Notably, over half of the gap tuning occurs within the narrow range of 20-24V.

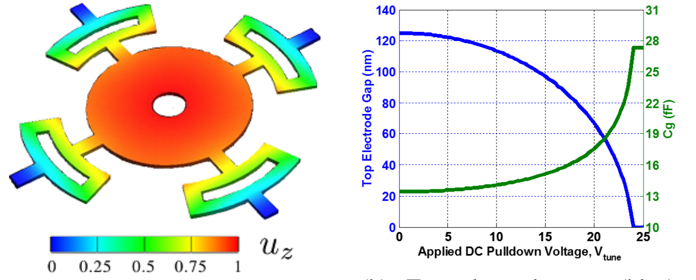

(a) A 3D rendering in COVENTOR of the chosen top electrode suspension design. The anchors of the structure are shown in blue. The color map indicates displacement u_z due to a downward force on the electrode.

(b) Top electrode gap (blue) and gap capacitance C_g (green) vs. V_{tune} for the suspension of Fig. 4a for a 1.6-µm-thick capacitive-piezo AlN disk resonator with 125 nm top and bottom gaps.

Fig. 4: Top electrode suspension (a) illustration and (b) displacement and capacitance vs. V_{tune} simulation.

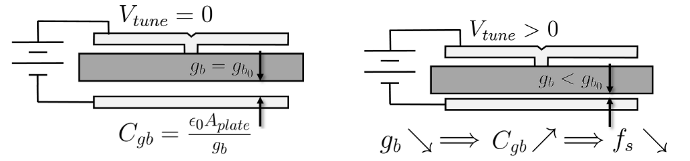

(a) An untuned top-electrode-supported bottom gap actuated resonator for which $V_{tune} = 0$ and for which bottom electrode vertical displacement is zero.

(b) A tuned resonator for which $V_{tune} > 0$ and for which nonzero resonator displacement causes gap reduction.

Fig. 5: Illustration of bottom gap tuning. Cross sections are included for an (a) untuned and a (b) tuned capacitive-piezoelectric AlN radial-contour-mode disk resonator using a top electrode anchor. Here, the bottom gap g_b is reduced by V_{tune}.

V. Top Gap Tuning vs. Bottom Gap Tuning

The device shown in Fig. 2 is an instance of a top gap tuned resonator, where the top electrode moves relative to the resonator. One can also make a bottom gap tuned resonator by anchoring the resonator to the top electrode rather than the substrate. Thus, when the top electrode descends, the resonator moves with it, and the bottom gap g_b changes, as is illustrated in Fig. 5. Here, a top electrode supported resonator allows for maximal electrode coverage and hence better electromechanical coupling and increased tuning range.

VI. Resonator Tuning Range

The available capacitive frequency tuning range for this device is the frequency difference between its minimum possible f_s, and maximum possible f_p values. Thus, to determine the largest tuning range one can attain, one can simulate the performance of a capacitive-piezo resonator with gaps reduced below 1 nm, yielding the gapless series resonance frequency, $f_{s,ng}$. As Eq. (6) shows, $C_x/2C_0$ for a resonator is

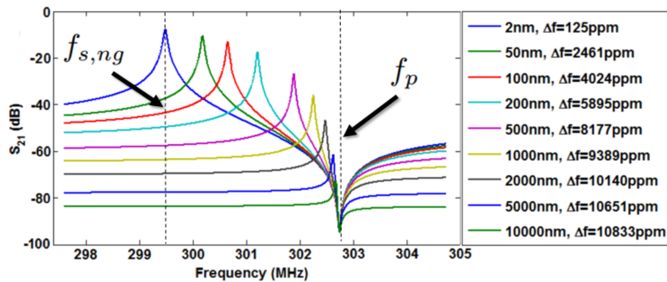

Fig. 6: Simulated gap reduction based frequency tuning for an 11.2-µm-radius, 1.6-µm-thick, AlN radial contour mode resonator demonstrating a maximum tuning range of ≈11,000 ppm. Nine frequency characteristics are shown at various values of g_{total} ranging from 2 nm to 10 µm.

a convenient expression for the maximum possible fractional tuning range.

$$\frac{\Delta f_{max}}{f_{s,ng}} = \frac{1}{2}\left(\frac{2(f_p - f_{s,ng})}{f_{s,ng}}\right) = \frac{1}{2}\frac{C_{x,ng}}{C_{0,ng}} \quad (6)$$

A. Simulation of Theoretical Maximum Tuning Range

Our model of the 300MHz 11.2-µm-radius capacitive-piezo disk of this work having full electrode coverage and 1 nm gaps predicts $C_x/C_0 = 2.2\%$. Thus, a maximum fractional frequency tuning range of 1.1% (11,000 ppm) is available. To illustrate the wide available tuning range, Fig. 6 presents multiple simulated S_{21} frequency characteristic plots for a capacitive piezo disk resonator having g_b=1nm and a widely actuatable top electrode gap, g_t. Here, g_t is varied from 1 nm to 10 µm. The plot legend lists the nine different values of total gap size included in the simulation and their corresponding frequency shifts from the zero gap state.

B. Constraints on Making Large Gaps for Tuning

Tuning with large gaps involves several undesirable tradeoffs. For example, excessive values of $g_{total} = g_t + g_b$, e.g., beyond 500 nm, can greatly diminish electromechanical coupling. Also, gap tuning efficiency, $\frac{d\Delta f_s}{dg_{total}}$, drops as g_{total} increases, eventually becoming quite small at large gap sizes. Gap tuning efficiency drops from 60 ppm/nm at 0 nm to only 3.8 ppm/nm at 500 nm. Third, accommodating a large range of motion would likely result in reduced fine gap tuning accuracy at small gap sizes. In view of these considerations, one should keep gap sizes below a judicious value of $g_{total,max}$.

C. Constraints on Making Small Gaps for Tuning

Choosing to fabricate capacitive-piezo resonators with very small gaps also involves undesirable tradeoffs. First, under imperfect deposition conditions, bending moments in AlN thin films can arise, typically causing structures to bend upward. Such strain gradients set a minimum limit on top gap sizes if electrode contact is to be avoided. Beyond stress concerns, reducing both g_b and g_t very aggressively may also lead to fabrication difficulties related to stiction, post-release cleaning, sacrificial layer pinholes, and/or surface roughness. Also, due

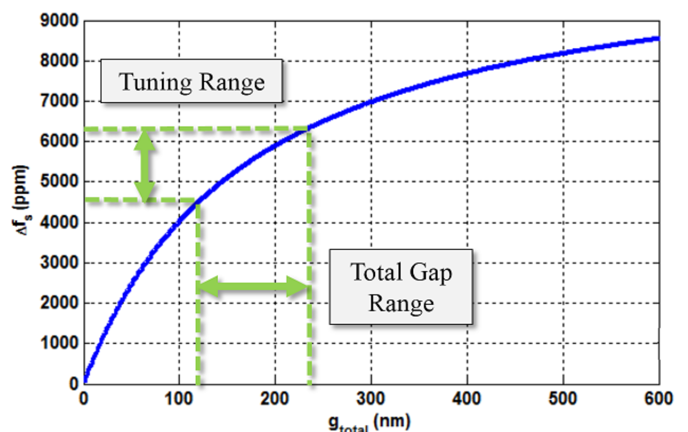

Fig. 7: Simulated fractional frequency shift from zero-gap state vs. g_{total} for an 11.2-µm-radius, 1.6-µm-thick, radial contour mode capacitive-piezo AlN resonator with reducable capacitive gaps. Included in the plot are annotations showing the achieved gap range of this work and its corresponding tuning range.

to the need to overetch AlN with the current fabrication process, a thick bottom sacrificial oxide eases concerns of excessively overetching the bottom electrode interconnect layer. One should thus avoid scaling g_{total} too aggressively simply to ensure proper operation.

D. Optimal Sizing of Gaps

In this work, top and bottom gaps of 120 nm were chosen to attain a respectable tuning range of ≈1,600 ppm without risking device failure. Here, the chosen tuning ratio, C_{max}/C_{min}, is 2. Larger tuning ratios are certainly possible. To examine the relationship between g_{total} and $\Delta f_s = f_s - f_{s,ng}$, refer to Fig. 7. Overlaid on the plot are annotations showing the designed gap range for our device and its associated tuning range of 1600 ppm. Considering possible future performance improvements, through using a wider range of g_{total} values, e.g., with a fixed g_b of 70 nm and a variable g_t between 0 nm and 430 nm, 5,200 ppm of tuning would be attained, representing a potential threefold improvement. Additional design iterations will determine the true limits of this technology.

VII. Dedicated Tuning Transducers

Two gap reduction based capacitive tuning methods are explored in this work: tuning through an input/output (I/O) transducer, which affects the I/O coupling, α, of Eq. (1); and tuning through a separate tuning transducer, which does not. Our analysis so far has emphasized tuning for single transducer devices for which I/O transduction and tuning transduction occur through the same electrode pair. Single transducer capacitive-piezo resonators advantageously minimize R_x and maximize C_x/C_0; however, the achieved values do not stay constant over the tuning range. If R_x and C_x/C_0 change too much through tuning f_s, some oscillator or filter designs may not function properly. Additionally, single transducer tuning

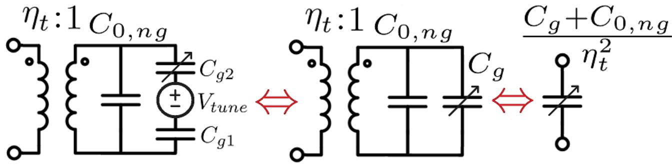

Fig. 8: Electromechanical circuit model for a dedicated capacitive piezo tuning element and its equivalent series compliance seen by $c_x = 1/k_r$, the inverse stiffness of the resonator.

often requires putting a tuning voltage in the I/O signal path, which can require a bias tee [6]. Using a dedicated tuning transducer outside the I/O signal path circumvents these issues, allowing one to tune f_s while R_x and C_x/C_0 stay constant.

A dedicated capacitive-piezo tuning element, the circuit model of which is shown in Fig. 8, allows a voltage controlled variable capacitance linked to an electromechanical transformer with transduction factor η_t to effectively act as a variable compliance, i.e., an inverse stiffness having units of [m/N]. This tuning element acts in series with the l_x, c_x, and r_x elements of Fig. 3a, adding to resonator stiffness. To calculate the frequency tuning for the overall resonator, simply substitute $c_{x,tuned}$ of Eq. (7) for c_x in both Fig. 3a and β of Eq. (2):

$$c_{x,tuned} = \frac{c_x(C_g + C_{0,ng})}{c_x\eta_t^2 + (C_g + C_{0,ng})} \tag{7}$$

As an example of the performance tradeoff of switching from I/O gap reduction based tuning to separated tuning, if the electrode configuration of a single transducer device is modified to instead allocate 50% of its area to dedicated I/O and 50% to dedicated tuning, hence reducing η and η_t, holding all else constant, R_x will increase by a factor of four and C_x/C_0 (and hence tuning range) will drop by a factor of two.

VIII. Device Fabrication

To validate the design and operation of the tunable capacitive-gap piezo resonators presented here, a number of such resonators were fabricated using a fabrication process similar to that of [6], though with several key improvements. Fig. 9 presents a cross section of a capacitive-piezo disk resonator. Here, the deposited film forming the bottom electrode was changed from the previously-used 150 nm thick molybdenum film to a 2µm-thick doped polysilicon film to avoid galvanic corrosion during a wet hydrofluoric acid release. The doped polysilicon is made relatively thick to reduce its sheet resistance to under 10 Ω/□. The large topography of the thick polysilicon was mitigated using a 2.5 µm oxide deposition which was then chemical mechanically planarized. The sacrificial oxide thicknesses were reduced down to 125 nm to improve C_x/C_0. Most importantly, the crystallinity of the reactively sputtered AlN film was dramatically improved, through proper chamber conditioning and heating the wafer during deposition, further increasing C_x/C_0. Using an X-ray diffractometer, the measured full-width half maximum of the AlN film used was measured at $1.60°$. Finally, the top electrode thickness was reduced, allowing for lower actuation voltages of the top electrode due to the strong cubic dependence of vertical stiffness on material thickness.

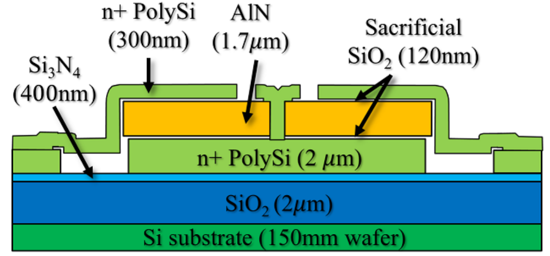

Fig. 9: A device cross-section illustrating materials used and their thicknesses.

IX. Experimental Results

We report experimental tuning demonstrations at 300 MHz of (a) a two transducer top-gap-tuned resonator to verify constant R_x tuning and (b) a single transducer bottom-gap-tuned resonator to verify maximum tunability and minimal R_x. Both devices were tested in a vacuum probe station using a properly calibrated network analyzer with a 50Ω termination at both ports. Transmission scattering parameter (S_{21}) measurements were collected and plotted for various values of V_{tune} to verify operation.

Fig. 10 demonstrates a two-disk device utilizing one electrode pair for I/O transduction and a separate electrode pair for top gap reduction tuning. As shown in the SEM, two radial contour-mode resonators are mechanically coupled using an extensional mode 800-nm-wide coupling beam of acoustic length λ/2 to form a single degree of freedom resonant system. The upper resonator is surrounded by an I/O transducer electrode pair through which its transmission vs. frequency is measured. Surrounding the lower resonator is the same tuning transducer shown in Fig. 8, consisting of a grounded bottom electrode and bias voltage (V_{tune}) actuated spring-supported top electrode. The measurement plot includes a series of 2-port transmission (S_{21}) measurements taken with various values of V_{tune} ranging from 0 to 24V. The entire frequency characteristic is shown to uniformly shift downward in frequency as V_{tune} is increased, with no changes in R_x, Q, and C_x/C_0, as expected.

Fig. 11 demonstrates tuning in a top-supported single-disk device with one transducer for both tuning and I/O in order to achieve maximum total tuning range. The measurement scheme for this device uses a bias tee to add a bias voltage to the RF input signal. As shown in the measurement plot, one achieves improved R_x, C_x/C_0, and tuning range through using a single transducer, as expected. Here, the measured tuning range is increased to 1547 ppm. The R_x of this device is showed to decrease as V_{tune} is increased, agreeing with the model. Note that f_p stays relatively fixed, as is simulated in Fig. 6.

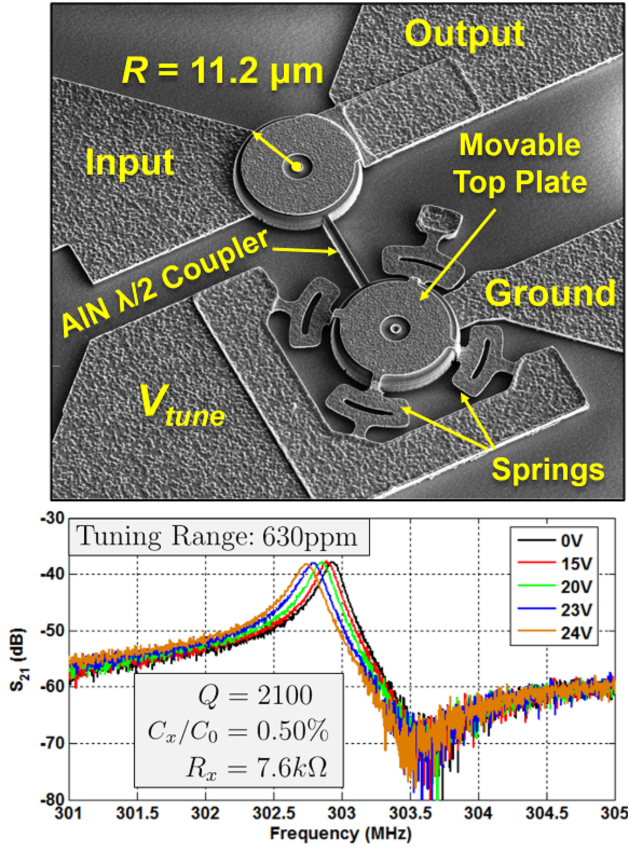

Fig. 10: Two transducer capacitive-piezo tuning demonstration.

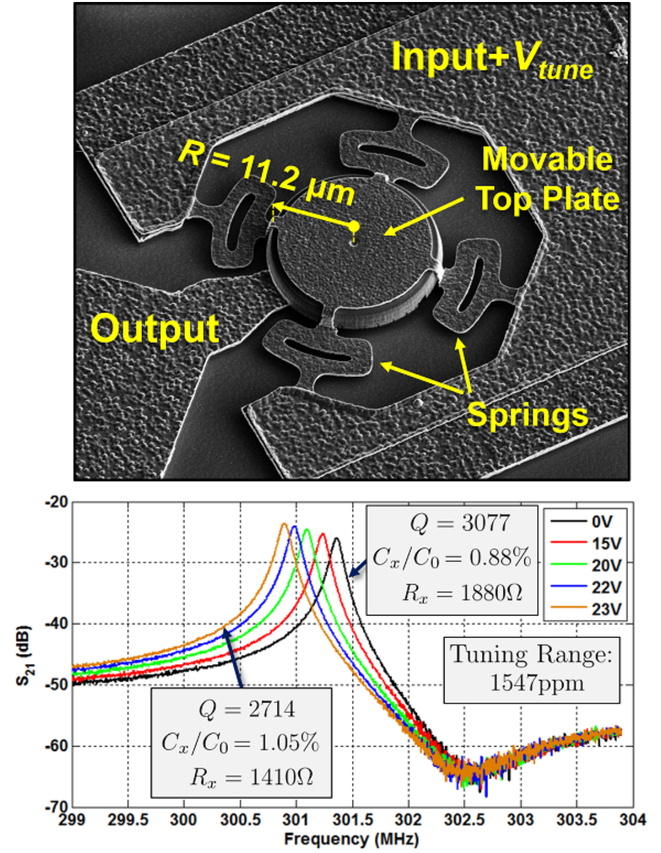

Fig. 11: Single transducer tuning demonstration.

A summary of capacitive-piezo tunable resonator model parameters that correctly predict tuning behavior of our demonstrated devices is included in Table I.

TABLE I: Tunable Resonator Model Parameters

Model Parameter	Single Disk Resonator	Two Disk Resonator
r_x	9.3×10^{-7} kg/s	2.75×10^{-6} kg/s
l_x	1.535×10^{-12} kg	3.070×10^{-12} kg
c_x	1.840×10^{-7} s^2/kg	9.20×10^{-8} s^2/kg
η, η_t	4.90×10^{-5} C/m	4.50×10^{-5} C/m
$C_{0,ng}$	$1.99 \times 10^{-14} F$	1.88×10^{-14} F
$g_{tot,IO}$ [min, max]	[136 nm, 240 nm]	[240 nm, 240 nm]
$g_{tot,tune}$[min, max]	(same as IO)	[150 nm, 240 nm]
α [max, min]	[0.56, 0.42]	[0.42, 0.42]
β [min, max]	[1.00488, 1.00639]	[1.0029, 1.0029]
$c_{x,tuned}/c_x$[min,max]	N/A	[0.9943, 0.9956]
Δf_s	-1510 ppm	-650 ppm

X. Conclusions

Voltage controlled gap reduction has now been shown as an effective means for controlling the resonance frequencies of capacitive-piezo AlN micromechanical resonators. Introducing integrated variable capacitances into VHF AlN resonators is also shown to enable higher Q's while maintaining strong coupling. We have demonstrated 1547 ppm of tuning at 300 MHz using a single transducer and 630 ppm of tuning using a dedicated tuning electrode to maintain constant R_x. Though these initial results are impressive, analysis shows that through optimizing gap sizes, a further threefold increase in the tuning range will be feasible. We believe that the tuning method presenting in this work will be useful for improving accuracy or reducing temperature induced frequency drift in our resonators, for which measured TCF's of 15 ppm/K are typical. Frequency modulation, mixing, passband correction of filters, and filter tunability may also be implemented using this technique.

Acknowledgment

The authors would like to thank DARPA, the Berkeley Sensor & Actuator Center, and the staff of the Berkeley Nanofabrication Laboratory for supporting this work.

References

[1] B. Kim, R. H. Olsson, and K. E. Wojciechowski, "Ovenized and thermally tunable aluminum nitride microresonators," *IUS* 2010, pp. 974-978.

[2] J. Hu, R. Parker, R. Ruby, and B. Otis, "A wide-tuning digitally controlled FBAR-based oscillator for frequency synthesis," *IFCS* 2010, pp. 608-612.

[3] B. Kim, R. Olsson, and K. Wojciechowski, "Capacitive frequency tuning of AlN micromechanical resonators," *Transducers* 2011, pp. 502-505.

[4] L.-W. Hung and C. T.-C. Nguyen, "Capacitive-piezoelectric AlN resonators with Q>12,000," *MEMS* 2011, pp. 173-176.

[5] T.-T. Yen., A. Pisano and C. T.-C. Nguyen, "High-Q Capacitive-Piezoelectric AlN Lamb Wave Resonators," *MEMS* 2013, pp. 114-117.

[6] R. A. Schneider and C. T.-C. Nguyen, "On/Off Switchable High-Q Capacitive-Piezoelectric AlN Resonators," *MEMS* 2014, pp. 1265-1268.